Proteasome Inhibition

DOI: 10.1002/anie.201000140

Elucidation of the Structure and Intermolecular Interactions of a Reversible Cyclic-Peptide Inhibitor of the Proteasome by NMR Spectroscopy and Molecular Modeling**

*Benjamin Stauch, Bernd Simon, Teodora Basile, Gisbert Schneider, Nisar P. Malek, Markus Kalesse, and Teresa Carlomagno**

Ubiquitin-dependent proteolysis is carried out by the proteasome,[1,2] a 0.7 MDa macromolecular machine consisting of four stacked heptameric rings.[3] In its central cavity, the proteasome carries two copies of three distinct active sites exerting caspase, trypsin, and chymotrypsin activity.[4–6] Owing to its ubiquity and generality, the proteasome plays a key role in diseases, such as cancer,[7] and the quest for novel proteasome inhibitors remains an evolving field.[8,9] Recently, a promising natural compound with antitumoral activity was described: argyrin, a cyclic heptapeptide from the myxobacterium *Archangium gephyra* (Scheme 1), interferes with tumor growth by stabilizing $p27^{KIP1}$ levels through proteasome inhibition.[10] We recently described the full synthesis of argyrin derivatives and their proteasome-inhibition profiles in vitro and in vivo.[11] Argyrin A shows similar potency to known proteasome inhibitors, such as bortezomib and MG-132,[9,12] but more specific and even better tolerated antitumoral activity in vivo. We have now solved the solution structure of argyrin A by NMR spectroscopy and report herein our investigations of its interaction with the proteasome by NMR spectroscopy and molecular modeling. We describe the spatial orientation of argyrin A in the active site of the proteasome, provide a rationale for the differential activity of argyrin analogues, and propose a structural basis for the functional activity of this potent proteasome inhibitor.

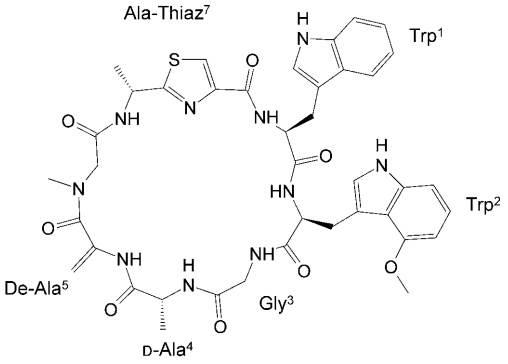

Scheme 1. Structure and configuration of argyrin A.

Argyrin A is a cyclic heptapeptide (Scheme 1) comprising tryptophan (Trp^1), a tryptophan derivative with a methoxy substituent at C4 of the indole (Trp^2), glycine (Gly^3), D-alanine (D-Ala^4), dehydroalanine (De-Ala^5) with an exocyclic double bond, sarcosine ($Sarc^6$), and a thiazole derivative of D-alanine (Ala-$Thiaz^7$).[13] First, we investigated the conformation of argyrin A in an aqueous environment by NMR spectroscopy. We observed a second set of resonances in non-crowded spectral regions with an intensity of about 10% of that of the main set of resonances. These additional resonances could result either from a second conformation of argyrin A or from degradation products. The absence of exchange peaks between the two sets of resonances in a ROESY experiment favors the second hypothesis.

We calculated 100 structures through the quantitative treatment of NOESY cross-peak intensities (mixing times: 80–300 ms; see Figure S1 in the Supporting Information) by using the full relaxation matrix approach[14] and a simulated annealing protocol. The structure calculation converged to a well-defined cluster of 11 low-energy structures (Figure 1; see also Figure S2 in the Supporting Information; average pairwise root-mean-square deviation (RMSD): 0.22 ± 0.09 Å). Excluding experimental restraints, the structure was minimized in explicit water; the low RMSD (0.52 Å) between the minimized and nonminimized structure indicated that the experimental structure was in a stable energy minimum.

The backbone of argyrin A adopts a compact conformation of dimensions $10 \times 6 \times 5$ $Å^3$, with residues De-Ala^5 and $Sarc^6$ bent out of the macrocycle plane by approximately 90° (Figure 1). The thiazole ring is coplanar with the adjacent

[*] B. Stauch, Dr. B. Simon, Dr. T. Basile, Priv.-Doz. Dr. T. Carlomagno
Structural and Computational Biology Unit
European Molecular Biology Laboratory (EMBL)
Meyerhofstrasse 1, 69117 Heidelberg (Germany)
Fax: (+49) 6221-387-8519
E-mail: teresa.carlomagno@embl.de
Prof. Dr. G. Schneider
Department of Chemistry and Applied Biosciences
Institute of Pharmaceutical Sciences, ETH Zürich
HCI H 411, Wolfgang-Pauli-Strasse 10, 8093 Zürich (Switzerland)
Prof. Dr. N. P. Malek
MHH-Klinik für Gastroenterologie, Hepatologie und Endokrinologie, Hannover (Germany)
Prof. Dr. M. Kalesse
BMWZ, Leibniz-Universität Hannover (Germany)
and
Helmholtz Zentrum für Infektionsforschung, 38124 Braunschweig (Germany)

[**] This research was supported by the EMBL. We acknowledge gratefully the excellent technical assistance of Frank Thommen and support from John P. Overington and the Cambridge Crystallographic Data Centre.

Supporting information for this article is available on the WWW under http://dx.doi.org/10.1002/anie.201000140.

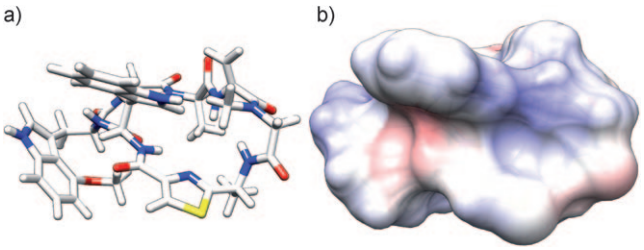

Figure 1. Solution structure of argyrin A: a) stick representation (C white, H white, N blue, O red, S yellow); b) with Coulomb electrostatics (blue: positive, white: neutral, red: negative) mapped onto the solvent-accessible surface.

peptide bond; this arrangement creates a planar constriction approximately parallel to the macrocycle plane. An additional constraint is introduced by the exocyclic methylene group, which probably restricts the dynamics of the macrocycle; a 1D proton spectrum of an argyrin analogue that lacks this moiety shows broadened resonances and additional peaks, both of which are indicative of a broader range of conformations sampled by the molecule. Whereas the methyl group attached to the N atom of Sarc[6] and the side chains of D-Ala[4] and Ala-Thiaz[7] are pointing inwards, carbonyl groups and the exocyclic methylene group point out of the macrocycle. The indoles assume a roughly perpendicular orientation (ca. 70°) and sandwich the peptide main chain.

Its high molecular weight excludes the eukaryotic S20 proteasome from NMR spectroscopic studies at room temperature. If argyrin forms a stable complex with the proteasome, the complex structure is not accessible by NMR spectroscopy. Crystallization of the proteasome with argyrin was attempted in a partner laboratory without success. However, if the dissociation of the argyrin/proteasome complex is fast enough ($k_{off} > 1\ ms^{-1}$), "transferred" techniques, such as transferred NOEs,[15] transferred cross-correlated relaxation rates,[16] and INPHARMA,[17,18] could be used to elucidate the protein-bound conformation of argyrin and its mode of binding to the proteasome.[19] Therefore, we tested whether transferred-NOE signals could be observed for argyrin upon addition of the proteasome. The observation of transferred NOEs would enable us to verify whether the proteasome-bound conformation of argyrin was similar to that found for the free ligand in solution. Unfortunately, only very weak transferred NOEs were observed for a 1:12.5 ratio of proteasome active sites to argyrin. Thus, the k_{off} rate of the complex is not fast enough on the time scale of NOESY experiments, and the protein-bound conformation of argyrin A is not directly accessible by NMR spectroscopy.

Next, we performed competition experiments to probe the binding site of argyrin by using the known proteasome β-subunit ligand MG-132 as a reporter for argyrin binding[9] (see the Supporting Information for details). Transferred NOE peaks of reasonable intensity were observed for a 1:12.5 mixture of proteasome active sites to MG-132; thus, the k_{off} value for the dissociation of the MG-132/proteasome complex is larger than $1\ ms^{-1}$, an observation that is in good agreement with previously reported data.[9] Upon titration of the sample with argyrin A, MG-132 cross-peak intensities were depleted significantly, which indicated efficient displacement of MG-132 from the canonical binding site by argyrin A. Although allosteric competition cannot be excluded, this result strongly suggests that argyrin A binds to the proteasome β subunits and might share the same binding site with MG-132.

To verify that argyrin A does not bind to the proteasome α subunit, we investigated the competition between argyrin A and chloroquine, a known ligand of the noncatalytic α subunit.[20] After preincubation of the proteasome with argyrin A, chloroquine was added to the sample. Chloroquine resonances exhibited strong transferred-NOE signals; these signals indicated that chloroquine can enter the proteasome cavity and bind to its binding site on the α subunit, which is evidently not occupied by argyrin A.

On the basis of the assumption that argyrin binds to the canonical catalytically active site on the proteasome β subunit, which is also occupied by MG-132 and bortezomib,[21] we set out to generate a model of the argyrin/proteasome complex by molecular modeling. To minimize the uncertainties in the modeling results, we assumed that the bioactive conformation of argyrin is similar to that found for the free peptide, on the basis of the rationale that the bioactive conformation of small molecules is usually highly favored in solution to minimize unfavorable energetic contributions upon binding.[22,23] As no crystal structure is available for the human proteasome, we "humanized" the three binding pockets of the yeast proteasome holo structure in a complex with bortezomib, a covalent inhibitor (PDB identifier 2F16[24]), by replacing diverging side chains in the yeast structure with the human equivalents (see Table S1 and Figure S3 in the Supporting Information), and docked argyrin A by using the program GOLD.[25] Protein side chains were kept flexible during docking to allow for adaptation of the binding site to the ligand. The conformation of the argyrin backbone was fixed to the solution conformation of the free ligand, whereas the Trp side chains were left free to adapt to the protein binding pocket (see the Supporting Information for details).

Since the different proteasome binding pockets have a common evolutionary origin, and argyrin A inhibits all catalytic functions comparably well (see Table S2 in the Supporting Information), we expected a common mode of binding to all three pockets. Along the same line, it has been proposed that docking robustness can be enhanced by docking different active analogues of one ligand to the same target to obtain a consensus binding mode.[26,27] Assuming that the correct binding mode is sampled at least once in every docking run, the intersection of all runs will contain the true binding mode; this procedure is expected to enhance both the specificity and the sensitivity of docking by compensating for inaccuracies in the starting structural models and weaknesses of the scoring function.

To apply the concept of the consensus binding mode, we docked four active argyrin derivatives (A, B, D, and F; see Table S2 in the Supporting Information) to the three different humanized proteasome binding pockets. The structures of argyrin derivatives B, D, and F were obtained by substitution of the corresponding functional groups in the solution

structure of argyrin A, followed by energy minimization to account for possible steric clashes. The resulting docking modes for all argyrin derivatives were clustered across binding pockets to obtain a consensus binding mode (see Figure S4 in the Supporting Information).

We obtained a single highly populated consensus binding mode for all pockets and all derivatives (Scheme 2; see also Figure S5 in the Supporting Information) and propose this binding mode to be representative of the argyrin/proteasome complex. A similar binding pose was found for docking to the yeast proteasome. For some pockets of the human proteasome and some argyrin derivatives (see Figures S4 and S6 in the Supporting Information), we obtained a second binding mode in which argyrin is flipped by approximately 180°; in this way, the interaction partners of Trp^1 and Trp^2 are effectively switched (see below).

In our model, argyrin A blocks the "specificity pocket" S1 close to the catalytic N termini of the proteasome (see Table S1 for a definition of the residues belonging to the S1 pocket); an excellent steric fit of the ligand to the binding pocket was observed, with residues Gly^3 and D-Ala^4 buried deeply inside the protein, whereas the thiazole group opposite is engaged in dispersive contacts with the pocket wall. Numerous interactions are conserved across the three pockets. Argyrin displays different polar, hydrophobic, and aromatic contacts with residues of the S1 pocket[28] and additional residues in close proximity. S1 residues 20, 22, and 27 participate in dispersive interactions with argyrin (Scheme 2; see also Figure S5 in the Supporting Information). Coordination of the carbonyl groups of Gly^3 and D-Ala^4 by hydrogen bonds to the NH group of the conserved residue G47 and the hydroxy group of T1 anchors argyrin to the bottom of the S1 pocket. In all three pockets, the backbone carbonyl group and the backbone NH group of T21 form hydrogen bonds to the backbone NH group and the carbonyl group of Trp^1 of argyrin. The positively charged N terminus of the protein is involved in a polar interaction with the carbonyl group of Sar^6. Besides these common features, the sidewall of the associated monomers (see Table S1 in the Supporting Information) contributes specific interactions with argyrin in the three different pockets. In the caspase pocket, Trp^1 and Trp^2 are sandwiched between M94 and H116, and H116 and Y114, respectively. The hydroxy group of S118 donates a hydrogen bond to the methoxy group of Trp^2. In the trypsin pocket, E22 and D114 coordinate the polar indole hydrogen atom of Trp^2, which is located inside a hydrophobic side pocket containing cysteine and methionine residues; Trp^1 contacts a hydrophobic patch around T48, L115, and I116. In the chymotrypsin pocket, the indole ring of Trp^2 occupies a side pocket formed by D114, S118, K125, A27, and the backbone of Y119. As in the caspase pocket, the hydroxy group of S118 donates a hydrogen bond to the methoxy group of Trp^2. The indole moiety of Trp^1 contacts a flat hydrophobic surface formed by residues G48, A49, and A50.

The natural derivatives argyrin A, B, C, D, and F are low-nanomolar inhibitors and were used to derive the consensus binding pose. None of the modifications would be expected to change the conformation of the argyrin backbone significantly. The binding pose shown in Scheme 2 was consistently found to be preferred in all three pockets for argyrin analogues B, D, and F. This consensus binding mode explains well the relative activity of the argyrin analogues in both in vitro tests and cell-based assays (see Table S2 in the Supporting Information). In argyrin B, elongation of the methyl side chain of D-Ala^4 by one carbon atom is well-tolerated in

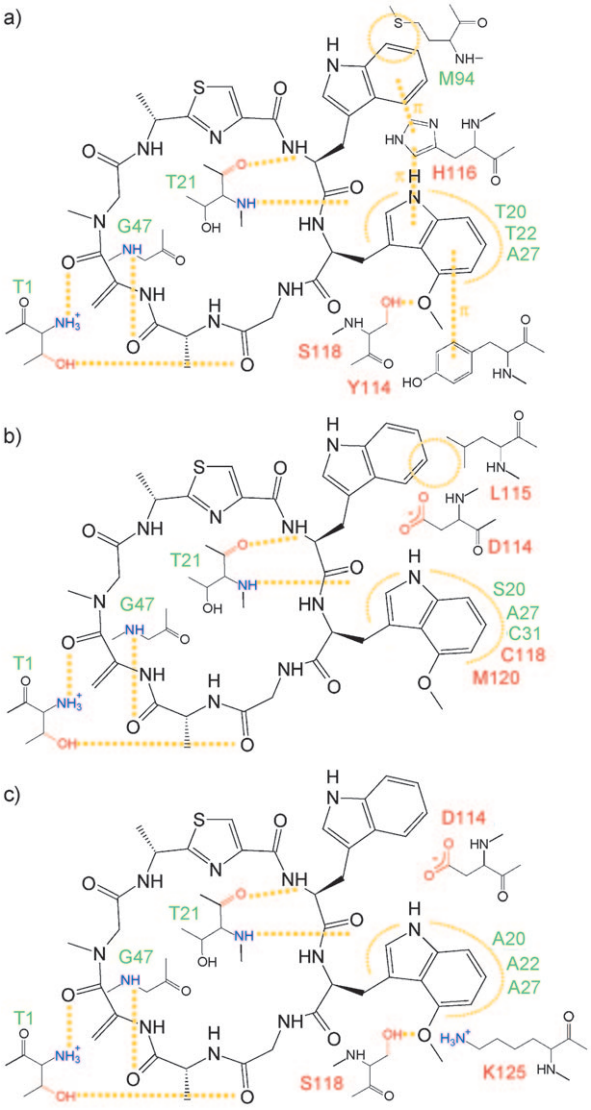

Scheme 2. Comparison of binding poses of argyrin with the proteasome: key interactions in a) a caspase-like binding pocket, b) a trypsin-like binding pocket, and c) a chymotrypsin-like binding pocket. Residues inside proteasome β subunits carrying the catalytic N teminus and residues in associated β subunits are labeled green and red, respectively (caspase: β6/β7, trypsin: β7/β3, chymotrypsin: β5/β1). See Figure S5 in the Supporting Information for a representation of the steric and electrostatic fit. Because of the relevance of the methoxy group of Trp^2 for the cellular activity of argyrin, the contacts formed by this group with the proteasome in the three pockets are summarized. In the caspase and chymotrypsin pockets, the hydroxy group of S118 forms a hydrogen bond with the methoxy group of Trp^2; in the trypsin pocket, where the detrimental effect of deleting OCH_3 is least, Trp^2 is coordinated stably in a hydrophobic side pocket formed by cysteine and methionine residues.

cellular assays. The longer side chain can be accommodated well in our docking mode, in which the side chain of D-Ala[4] points in the direction of the deep S1 cleft below the macrocycle plane.

In argyrin D, the additional methyl group at the C^{δ} position of Trp^2 is likely to restrict the conformational space accessible to the side chain of Trp^2. The activity profile of argyrin D is identical to that of argyrin B; in agreement, in our model, the conformation of the Trp^2 indole is such that the additional methyl group can be readily accommodated without changes in the orientation.

Most interestingly, the activity of argyrin F, in which the methyl carbon atom of Ala-Thiaz[7] is substituted with an additional OH group, is higher than that of argyrin A. This improvement in activity cannot be explained by the better solubility of argyrin F with respect to that of argyrin A, as the introduction of hydrophilic functionalities at other positions does not cause the same increase in activity.[11] In our model, the hydroxy group of Ala-Thiaz[7] in argyrin F forms a hydrogen bond with the carbonyl group of the conserved residue G23 and thus contributes directly to the stability of the complex.

Comparison of the activity of other analogues revealed that the introduction of a methyl group on the C^{α} atom of Gly^3 is well-tolerated in the pro-*R* position but detrimental in the pro-*S* position (see Table S2 in the Supporting Information). In our structure of argyrin A, steric hindrance between a methyl group in the pro-*S* position and the carbonyl group of Trp^2 would distort the conformation of the macrocycle. Furthermore, in our docking model, a pro-*S* methyl group would clash with the protein backbone close to residue 20 in the trypsin and chymotrypsin pockets, whereas a pro-*R* methyl group would protrude further into the S1 cleft (see Figure S7 in the Supporting Information). Another argyrin analogue lacking the *exo*-methylene group of De-Ala^5 displayed significantly less activity (see Table S2 in the Supporting Information). The removal of this structural constraint dramatically increases the flexibility of the macrocycle and changes the conformational landscape of the molecule, as shown by the large differences between this analogue and argyrin A in both the line width and the chemical shift of their NMR resonances (data not shown). Thus, the binding of this analogue without the *exo*-methylene group to the proteasome is likely to be entropically disfavored.

Notably, the presence of the methoxy group on the side chain of Trp^2 is essential for activity in all pockets, as indicated by a considerable loss of activity for argyrin E, which lacks this group, and for other derivatives without this group (see Table S2 in the Supporting Information). In our docking model, this methoxy group is involved in several interactions with protein side chains of both dispersive and electrostatic character. However, the interactions are not fully conserved across the pockets as a result of poor conservation of the proteasome sequence in the stretch close to Trp^2 (Scheme 2). In the caspase and chymotrypsin pockets, the methoxy oxygen atom is in a favorable position to form H bonds to the hydroxy group of S118, but in the trypsin pocket no H bond can be formed. However, it has been reported[9] that the chymotrypsin-like activity is the most relevant for proteasome function, and that impairment of this pocket, either by point mutations or by selective inhibition, also influences the activity of the other pockets. Thus, it is conceivable that at a molecular level, the lack of the methoxy group is particularly deleterious for the inhibition of the chymotrypsin pocket activity, and that this negative effect is transferred to the trypsin pocket through a still unknown allosteric mechanism.

In summary, we applied NMR spectroscopy and molecular docking to study the mode of interaction of argyrin, a promising novel anticancer agent, with the proteasome. We obtained an experimental NMR structure of the ligand in a polar solution and docked this structure to the β ring of the proteasome, following NMR spectroscopic experiments that indicated the competitive binding of argyrin and the known β-ring ligand MG-132. We presented evidence that argyrin can interact tightly with the canonical substrate-binding site of the proteasome and thereby prevent substrate degradation. Furthermore, we presented an atomic-interaction model in faithful agreement with structure–activity-relationship data. Interestingly, besides numerous conserved backbone interactions between argyrin and all three substrate-binding pockets and a large number of hydrophobic interactions, we found versatile specific contacts between the two aromatic tryptophan moieties of argyrin and variable regions of the proteasome binding pocket. These contacts might facilitate rational substitution of the ligand to enable proteasome-subunit specificity.

Experimental Section

Sample preparation: For structure determination, argyrin A was reconstituted to a final concentration of 500 μM in a mixture of 70% H_2O/D_2O and 30% [D_6]dimethyl sulfoxide (DMSO). Purified yeast S20 proteasome was a kind gift of Michael Groll, TU Munich (Germany). For interaction experiments, a solution of the S20 proteasome in aqueous (H_2O) buffer (20 mM Tris-Cl (made from 2-amino-2-hydroxymethylpropane-1,3-diol and HCl), 1 mM ethylenediaminetetraacetic acid, 450 mM NaCl) was exchanged for an equivalent D_2O buffer by dialysis three times over a 10 K membrane. After solvent exchange, an argyrin solution in [D_6]DMSO was added to a final total percentage of DMSO of 30% v/v. The final concentration of S20 proteasome active sites was 20 μM. For competition experiments, MG-132 (250 μM) was added, and a concentrated solution of argyrin A (10 mM) in [D_6]DMSO was titrated into the mixture to argyrin A/MG-132 molar ratios of 1:4 and 1:2.

NMR spectroscopy and structure calculation: NMR spectra were recorded on Bruker Avance spectrometers operating at 500, 600, 800, and 900 MHz and equipped with cryogenic probe heads. For the assignment of argyrin A resonances, HSQC, COSY, TOCSY, and NOESY spectra were recorded. For structure determination, a series of NOESY experiments were carried out at 298 K with mixing times of 80, 100, 200, and 300 ms. For argyrin A/proteasome interaction experiments and argyrin A/MG-132 competition experiments, one-dimensional and two-dimensional NOESY spectra were recorded at a constant mixing time (300 ms) at each step of the titration. The structure of argyrin was calculated with XPLOR-NIH 2.13 by using a restrained simulated annealing protocol and the full relaxation matrix approach starting from a single template structure. By employing the same force field but excluding experimental restraints, the resulting structure was energy-minimized for 10000 steps in explicit water.

Molecular modeling of the human S20 proteasome: Human reference protein sequences were aligned to their corresponding yeast homologues. Nonidentical positions in the alignment that mapped to positions within 10 Å of bortezomib in the holo structure of the yeast S20 proteasome cocrystallized with bortezomib (PDB 2F16) were selected, and amino acids of the yeast crystal structure were substituted with the human equivalents. Ligands were removed, hydrogen atoms were added, and substituted side chains were energy-minimized to yield the "humanized" S20 proteasome binding sites.

Molecular docking and binding-mode extraction: Argyrin A and some of its analogues were docked to yeast and "humanized" binding sites by using GOLD 4.0 and scored by GoldScore. The binding site was defined as an area with a diameter of 10 Å around the coordinate of the center of bortezomib in PDB 2F16. Side chain torsional angles and the position of the C^{α} atom of amino acids in the bortezomib binding pockets were kept flexible by employing a rotamer library to emulate induced fit. Docking parameters were set to "auto", search efficiency to "2". The ligand main-chain ring was kept fixed to the experimental conformation, whereas the ligand side chains were fully flexible throughout the docking. A total of 100 docking solutions were computed per ligand and binding pocket; binding pockets were superimposed, and ligand solutions were clustered hierarchically by using single-linkage clustering and a cutoff of 3.0 Å RMSD for the main-chain atoms. Average coordinates of the main-chain ring were computed for each ligand cluster, and the solution with a minimal RMSD from this average was regarded as cluster-representative. To extract a common binding mode for each ligand in the three pockets, we compared cluster representatives for one pocket with the cluster representatives of the other two pockets for every pocket in turn; when the main-chain RMSD was lower than the cutoff used for the initial clustering, binding modes were considered to be identical.

Received: January 9, 2010
Revised: March 16, 2010
Published online: April 20, 2010

Keywords: cancer · competitive binding · ligand interactions · NMR spectroscopy · proteasomes

[1] W. Baumeister, J. Walz, F. Zühl, E. Seemüller, *Cell* **1998**, *92*, 367.
[2] O. Coux, K. Tanaka, A. L. Goldberg, *Annu. Rev. Biochem.* **1996**, *65*, 801.
[3] S. Murata, H. Yashiroda, K. Tanaka, *Nat. Rev. Mol. Cell Biol.* **2009**, *10*, 104.
[4] C. S. Arendt, M. Hochstrasser, *Proc. Natl. Acad. Sci. USA* **1997**, *94*, 7156.
[5] W. Heinemeyer, M. Fischer, T. Krimmer, U. Stachon, D. H. Wolf, *J. Biol. Chem.* **1997**, *272*, 25200.
[6] A. F. Kisselev, A. Callard, A. L. Goldberg, *J. Biol. Chem.* **2006**, *281*, 8582.
[7] J. B. Almond, G. M. Cohen, *Leukemia* **2002**, *16*, 433.
[8] A. S. Eustáquio, B. S. Moore, *Angew. Chem.* **2008**, *120*, 4000; *Angew. Chem. Int. Ed.* **2008**, *47*, 3936.
[9] A. F. Kisselev, A. L. Goldberg, *Chem. Biol.* **2001**, *8*, 739.
[10] I. Nickeleit, S. Zender, F. Sasse, R. Geffers, G. Brandes, I. Sörensen, H. Steinmetz, S. Kubicka, T. Carlomagno, D. Menche, I. Gütgemann, J. Buer, A. Gossler, M. P. Manns, M. Kalesse, R. Frank, N. P. Malek, *Cancer Cell* **2008**, *14*, 23.
[11] L. Bülow, I. Nickeleit, A.-K. Girbig, T. Brodmann, A. Rentsch, U. Eggert, F. Sasse, H. Steinmetz, R. Frank, T. Carlomagno, N. P. Malek, M. Kalesse, *ChemMedChem* **2010**, *5*, 716.
[12] J. Adams, M. Behnke, S. Chen, A. A. Cruickshank, L. R. Dick, L. Grenier, J. M. Klunder, Y. T. Ma, L. Plamondon, R. L. Stein, *Bioorg. Med. Chem. Lett.* **1998**, *8*, 333.
[13] F. Sasse, H. Steinmetz, T. Schupp, F. Petersen, K. Memmert, H. Hofmann, C. Heusser, V. Brinkmann, P. von Matt, G. Hofle, H. Reichenbach, *J. Antibiot.* **2002**, *55*, 543.
[14] M. Nilges, J. Habazettl, A. T. Brunger, T. A. Holak, *J. Mol. Biol.* **1991**, *219*, 499.
[15] P. Balaram, A. A. Bother-By, J. Dadok, *J. Am. Chem. Soc.* **1972**, *94*, 4015.
[16] B. Reif, M. Hennig, C. Griesinger, *Science* **1997**, *276*, 1230.
[17] J. Orts, J. Tuma, M. Reese, S. K. Grimm, P. Monecke, S. Bartoschek, A. Schiffer, K. U. Wendt, C. Griesinger, T. Carlomagno, *Angew. Chem.* **2008**, *120*, 7850; *Angew. Chem. Int. Ed.* **2008**, *47*, 7736.
[18] V. M. Sánchez-Pedregal, M. Reese, J. Meiler, M. J. Blommers, C. Griesinger, T. Carlomagno, *Angew. Chem.* **2005**, *117*, 4244; *Angew. Chem. Int. Ed.* **2005**, *44*, 4172.
[19] T. Carlomagno, *Annu. Rev. Biophys. Biomol. Struct.* **2005**, *34*, 245.
[20] R. Sprangers, X. Li, X. Mao, J. L. Rubinstein, A. D. Schimmer, L. E. Kay, *Biochemistry* **2008**, *47*, 6727.
[21] L. J. Crawford, B. Walker, H. Ovaa, D. Chauhan, K. C. Anderson, T. C. Morris, A. E. Irvine, *Cancer Res.* **2006**, *66*, 6379.
[22] M. Erdélyi, B. Pfeiffer, K. Hauenstein, J. Fohrer, J. Gertsch, K. H. Altmann, T. Carlomagno, *J. Med. Chem.* **2008**, *51*, 1469.
[23] M. Marraud, A. Aubry, *Biopolymers* **1996**, *40*, 45.
[24] M. Groll, C. R. Berkers, H. L. Ploegh, H. Ovaa, *Structure* **2006**, *14*, 451.
[25] M. L. Verdonk, J. C. Cole, M. J. Hartshorn, C. W. Murray, R. D. Taylor, *Proteins Struct. Funct. Genet.* **2003**, *52*, 609.
[26] M. Barker, M. Clackers, R. Copley, D. A. Demaine, D. Humphreys, G. G. Inglis, M. J. Johnston, H. T. Jones, M. V. Haase, D. House, R. Loiseau, L. Nisbet, F. Pacquet, P. A. Skone, S. E. Shanahan, D. Tape, V. M. Vinader, M. Washington, I. Uings, R. Upton, I. M. McLay, S. J. Macdonald, *J. Med. Chem.* **2006**, *49*, 4216.
[27] M. Barker, M. Clackers, D. A. Demaine, D. Humphreys, M. J. Johnston, H. T. Jones, F. Pacquet, J. M. Pritchard, M. Salter, S. E. Shanahan, P. A. Skone, V. M. Vinader, I. Uings, I. M. McLay, S. J. Macdonald, *J. Med. Chem.* **2005**, *48*, 4507.
[28] M. Groll, L. Ditzel, J. Löwe, D. Stock, M. Bochtler, H. D. Bartunik, R. Huber, *Nature* **1997**, *386*, 463.

